CBN-07-10

A Quick, Cheap, Rearranged-CESR Route to the Brilliance Frontier

Richard Talman
Cornell Laboratory of Elementary-Particle Physics

August 9, 2007

Abstract

A plan is given to reconfigure the existing components of CESR into a high brilliance x-ray source in the Wilson tunnel. The design conserves the ring footprint and the 5 GeV electron energy, and (initially) uses the same filling sequence as the present ring. To exceed the performance of existing sources, it is necessary to accommodate the long undulators that were not envisaged when existing rings (except SPRING-8) were designed. Fortuitously, the existing straight section structure of the Wilson tunnel makes this possible. Because of its relatively large circumference and relatively high energy, after this upgrade the lab will join the frontier for *high energy* x-rays currently served only by the APS at Argonne, ESRF in France, and SPRING-8 in Japan. The challenge is to join this group for routine studies and to exceed them in selected areas.

The billions of dollars currently being spent worldwide on many new x-ray sources testify to the timeliness of the x-ray science the upgraded CESR would enable. For hard x-rays (used, or example, for coherent imaging of thick samples, which is one of exciting new prospects) the upgraded CESR can far exceed the capabilities of all facilities presently under construction.

Tentative cost estimates are given; they are based on the costs that would have been incurred at the time CESR was first constructed, inflated by the nominal cost-of-living factor since then. Irrespective of the (large) uncertainty in the value of this inflator, the conversion cost will be small compared to the value of the existing CESR infrastructure (assessed on the basis of replacement cost.) In other words the upgrade represents great value for a commodity in great demand aroung the world, and one that can put Cornell on the brilliance frontier within a few years.

On a longer time scale the lab plans to also join the fast timing frontier by developing a high brightness, full energy cryogenic linac and energy recovery linac. The reconfiguration described here will provide beam lines needed for the ultrafast timing experiments, and possibly higher brilliance, that will become possible when these sources are available.

1 Introduction and Design Considerations

Three candidate CESR upgrade options (one combined function and two separated function) were subjected to preliminary investigation that was described in an earlier (unpublished) report and presented in a Feb. 2, 2007, Journal Club presentation, Of the three options, the one labeled **C**, the combined function option, though slightly the most expensive, was subsequently judged to be substantially the best, and is the only option discussed in this report.

A large degree of arbitrariness remains, especially concerning the precise layout of x-ray lines. For the sake of definiteness the insertion device sources for all beam lines are assumed to be undulators, sectioned into lengths that are even multiples of about 2.5 m. If desired any such line can be split into a pair of lines as at the Argonne APS. Those lines directed at the present laboratory building are emphasized (especially those along existing CHESS lines). These lines are referred to as "visible" or as "instrumented" in tables below. (To develop the many other potential sources, labelled "free", would require tunnelling.) Clearly these assignments are somewhat arbitrary so far. Of the tentatively instrumented lines, six are somewhat superior in that they have exactly zero dispersion and 3.2 nm horizontal emittance. Nine of the visible beam lines have approximately 6 nm "effective" horizontal emittance; (The increase from 3.2 nm accounts for their average dispersion of roughly 0.15 m); these are referred to as "utility" lines. The two $D = 0$, $\epsilon_x = 3.2\,\mathrm{m}$ lines supporting especially long undulators will have brilliances exceeding current world standards.

These features will put the ring on the brilliance frontier immediately, but the fast-timing frontier will await the full-energy, low emittance linac currently under development. All or most of the beam lines described in this paper will be able to fully exploit subpicosecond, reduced emittance bunches once they have become available from that linac.

During the time interval before that linac becomes available injection will be from the existing synchrotron. During this phase limited injection rate may limit the brilliance because of beam lifetime reduction due to the Touschek effect. When the linac is available it will be an ideal injector and will be expected to give a substantial increase in integrated brilliance.

One wishes, to the extent possible, to use existing storage ring components. As well as reducing cost this will provide the advantage of familiarity and avoid the need for new designs. For the design described here it will be possible, for the most part, to preserve iron magnets, but their coils will have to be rebuilt. In the case of dipoles this is because of the decreased bend radius required (about 45 m instead of 89 m) and their "chevron" paired magnet coil design. Because of the combined function design, new dipole laminations will be required. New coils are required for the quadrupoles because their required focal strengths are somewhat greater than the maxima imposed by the existing coils. For the same reason (more quads per cell) a substantial number of new quadrupoles (assumed to be of the same design) will be required. In all cases the existing magnets are far from iron saturation and the maximum excitations are governed by cooling considerations.

To constrain the design, various constraints were imposed in the earlier investigation: all magnet dimensions retained; perfect sextant symmetry, common powering of all magnets (of the same type); 768 m circumference; $D = 0$ in all straight sections, and identical FODO sections in all drifts. In this follow-up study, to enable North and South halves to be different, the sextent symmetry requirement was dropped. Because the lattice closure is therefore no longer guaranteed by symmetry, the North straight section was replaced by a three FODO cell "trombone section" of length imposed by closure. This fitting was done only after the standard FODO cells were distributed to match existing CHESS lines, and to keep the lattice footprint close to its required location. This fit is shown in Fig. 3. (A final trimming of this fit will use the horizontal steering coils each bend magnet will have for horizontal steering.) Failure to meet any one of these constraints (except fitting in the tunnel) would have willingly been dropped but, as it happens, the constraints have been met fairly easily.

The theoretically-assured, ultrasmall emittance will only be achieved with far more careful lattice tuning than has been necessary with CESR in the past. This is primarily because of the extremely small dispersion values. It was for this reason that the lattice has been constrained to be so simple. The entire lattice is constructed from the three "LEGO block" segments illustrated in Fig. 2. Except for construction errors, the optics will be the identical wherever these segments appear. Of course small errors will be inevitable, and the otherwise exactly equal currents in the quadrupoles will have to be trimmed operationally.

It might be thought that the CESR equilibrium emittance could not be greatly affected by simply rearranging the same components, from its present FODO configuration to (approximately) minimum-emittance design. To the contrary, the equilibrium emittance can be reduced by almost two orders of magnitude. Along with longer undulators, this can give more than four orders of magnitude increase in the x-ray brilliance. Even more than eliminating the strong bends (originally required to provide separation for the colliding beam detectors) the single most important emittance reduction comes from the reduction of maximum dispersion from a few meters to 20 centimeters. Also, realizing that, in the present CESR FODO lattice, there are two full chevron bends per cell, but only one in the proposed design, the possibility of great emittance reduction may seem more credible.

Design of minimum emittance lattices is described in considerable detail in Chapter 11 of my book "Accelerator X-Ray Sources".[1]. The achievable parameters resemble the values given in the $L_C = 15m$ column of Table 11.1. Fig. 1 below, with notation adapted to the current design, is copied from Fig. 11.9. Numerous articles in CERN Yellow Report CERN-8-04[3], especially the section due to Ropert[4], are also very useful. Numerous other useful articles are given in the bibliography.

I have not slavishly attempted to meet the minimum emittance condition exactly. One might think that setting $D = 0$ at bend centers would lead to minimum emittance, but that is not quite true. There is a nice plot (Fig. 7) by A. Streun in CERN Yellow Report, CERN-2005-012[5], that shows the emit-

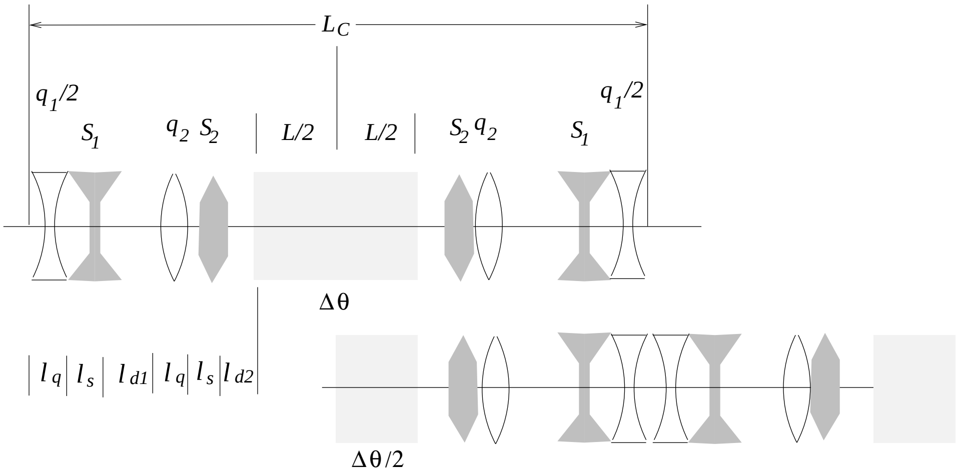

Figure 1: Element lengths and strengths for one achromatic cell. The lower element ordering is convenient for relating design values of β_0 and D_0 (at the center of the bend) to the Twiss functions of sectors consisting of repeated cells. However $q_1/2$ is half of a quad shared with the adjacent sector. The rectangular shaded region represents a (combined function) bend magnet and the angular figures represent sextupoles. As the lenses are drawn, it is horizontal optics being illustrated.

tance penalty (away from minimum) resulting from not quite optimal values of D and of β_x. I have considered it far more important to maintain the $D = 0$ condition rigorously in all straight sections. This has made it very convenient to set $D = 0$ also at the center of every bend. (By shifting the positions of the half-bends at sextant ends this can perhaps be relaxed, but I have not tried to do it.)

In fact, it has seemed to me appropriate to maximize the available straight section length (available for undulator insertion devices and other required equipment) and to assure conservative, flexible operation, even at the expense of modest increase of emittance. The choice among the options is therefore based primarily on x-ray beam line considerations. By taking up a larger fraction of the ring with bending magnets the equilibrium emittance could be reduced but the result would be reduced cumulative brilliance because of the loss of circumferential space available for undulators.

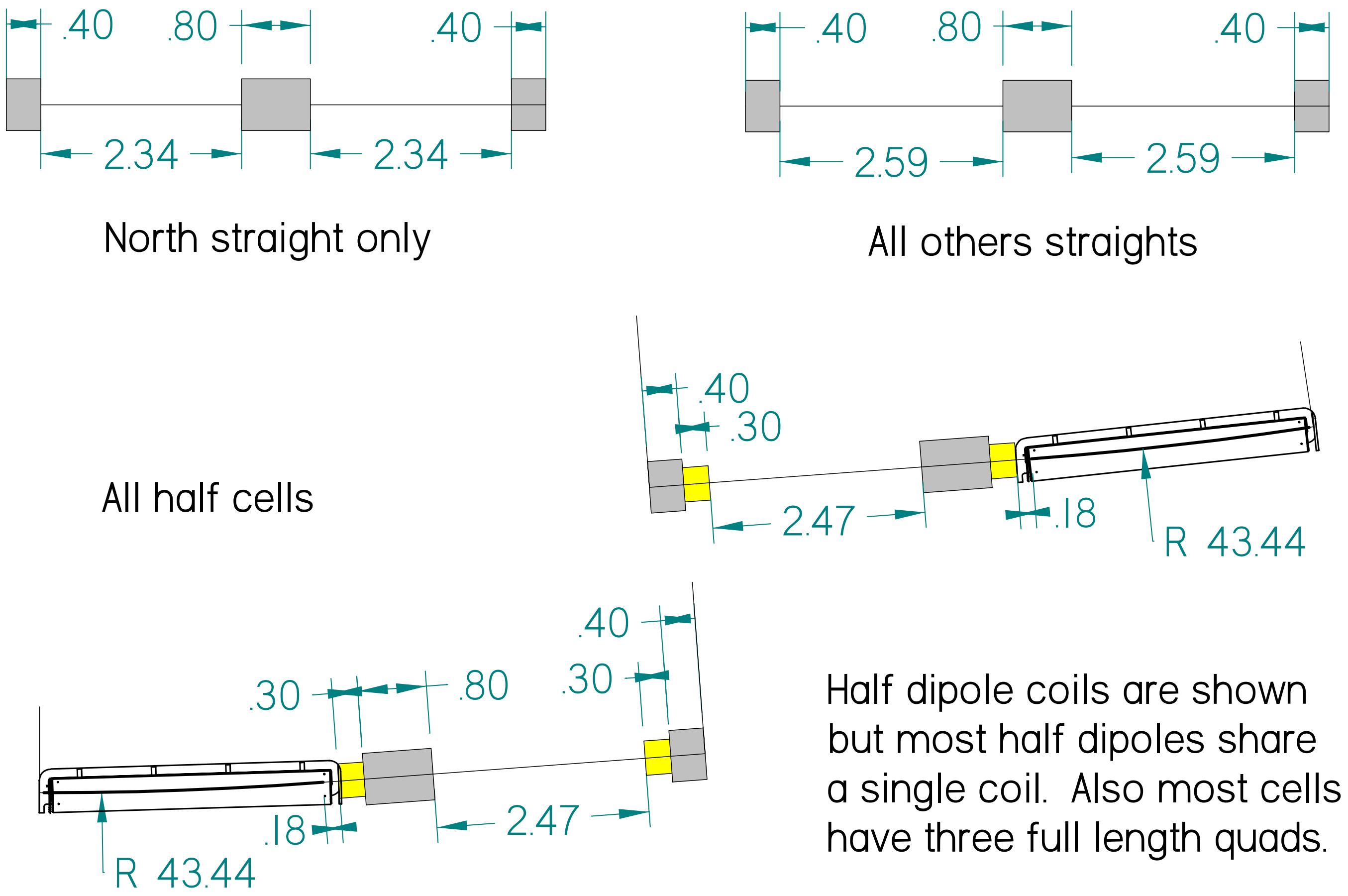

Figure 2: All the “LEGO blocks” needed to construct the lattice. More accurate lengths are given in tables.

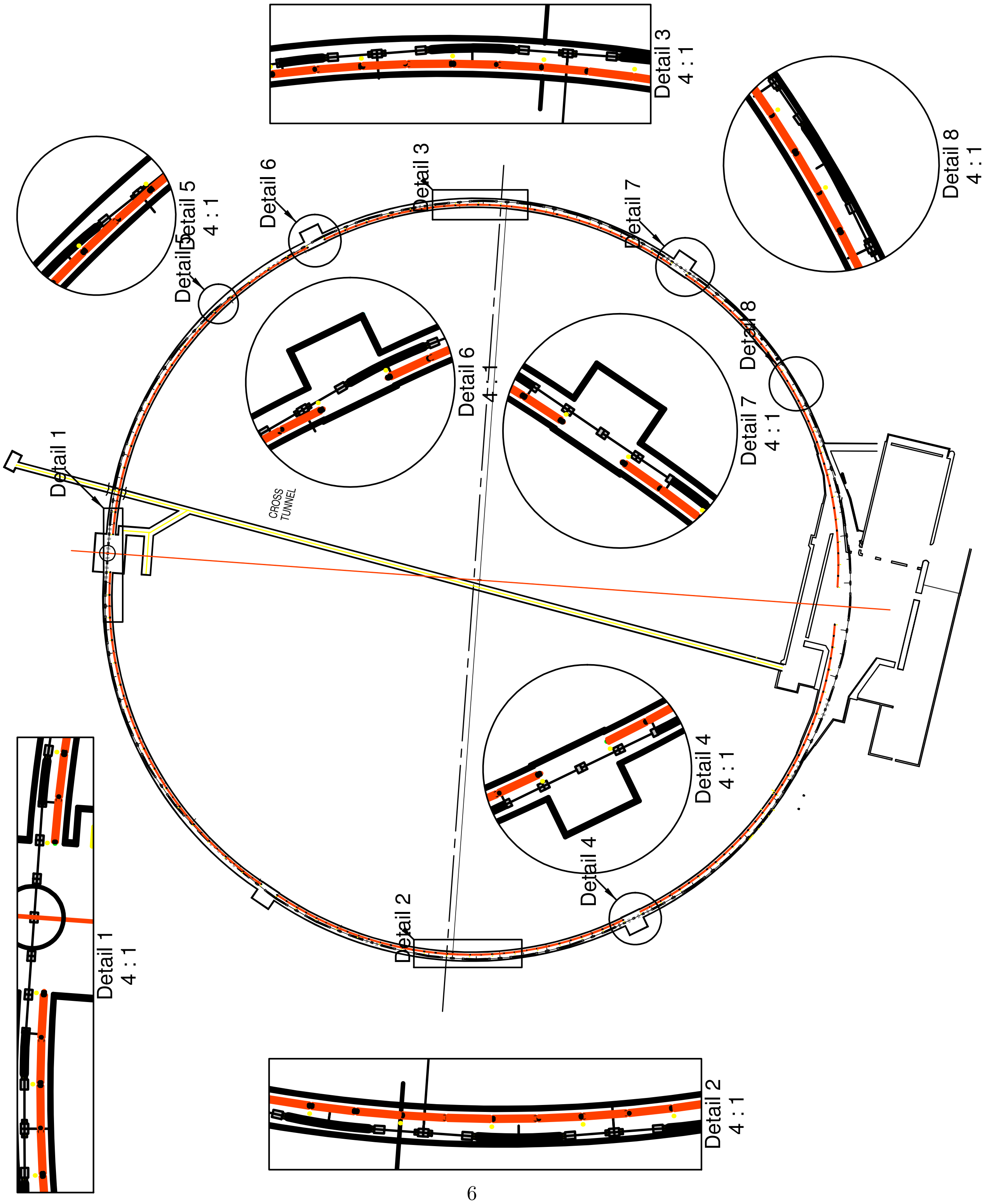

Figure 3: Synchrotron and (not yet exactly positioned) light source fit into the Wilson tunnel.

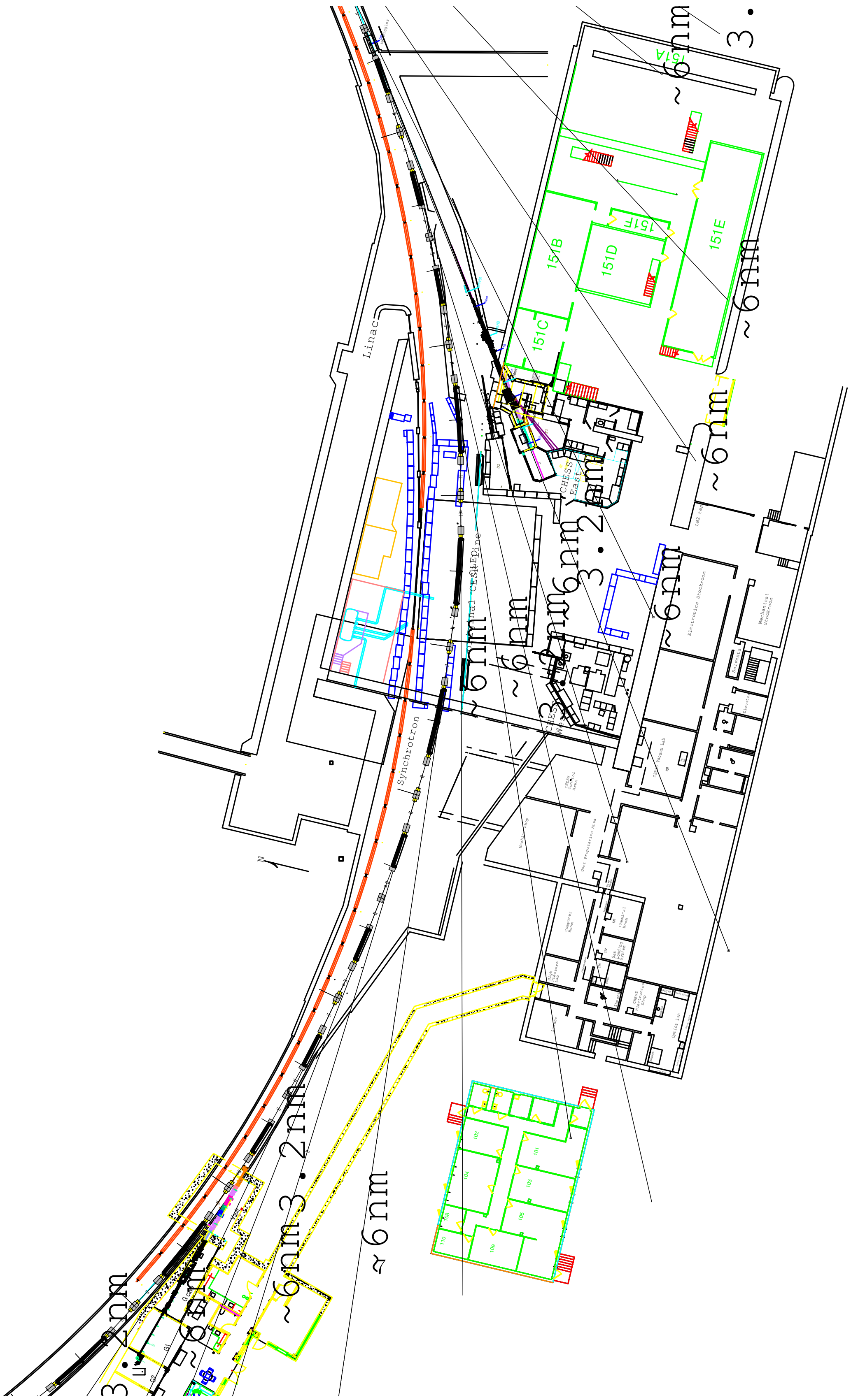

Figure 4: Beam lines impinging on present Wilson Lab experimental hall.

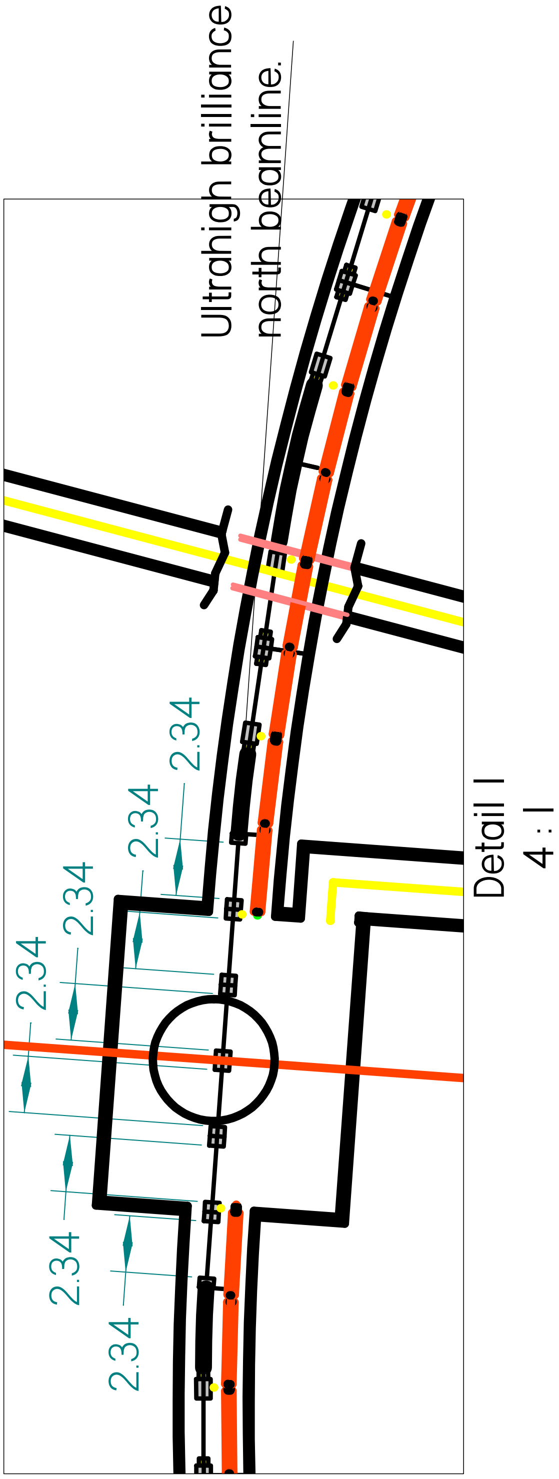

Figure 5: Detail view (from earlier figure) showing the maximum brilliance, 14 m undulator, north area beamline source.

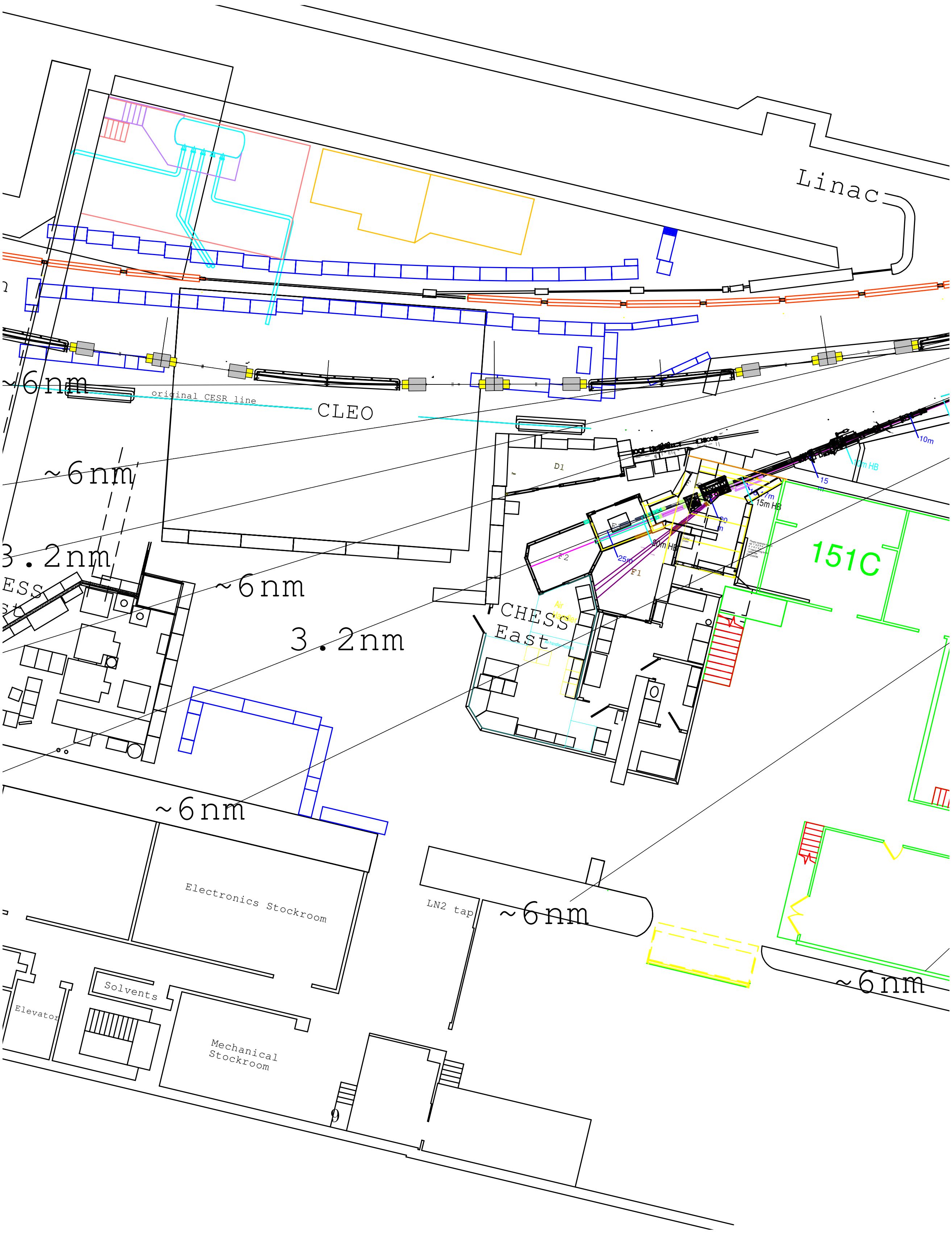

Linac
~6nm
original CESR line
CLEO
~6nm
3.2nm
~6nm
D1
CHESS
East
3.2nm
151C
~6nm
Electronics Stockroom
LN2 tap
~6nm
~6nm
Solvents
Elevator
Mechanical
Stockroom
15m HB
10m

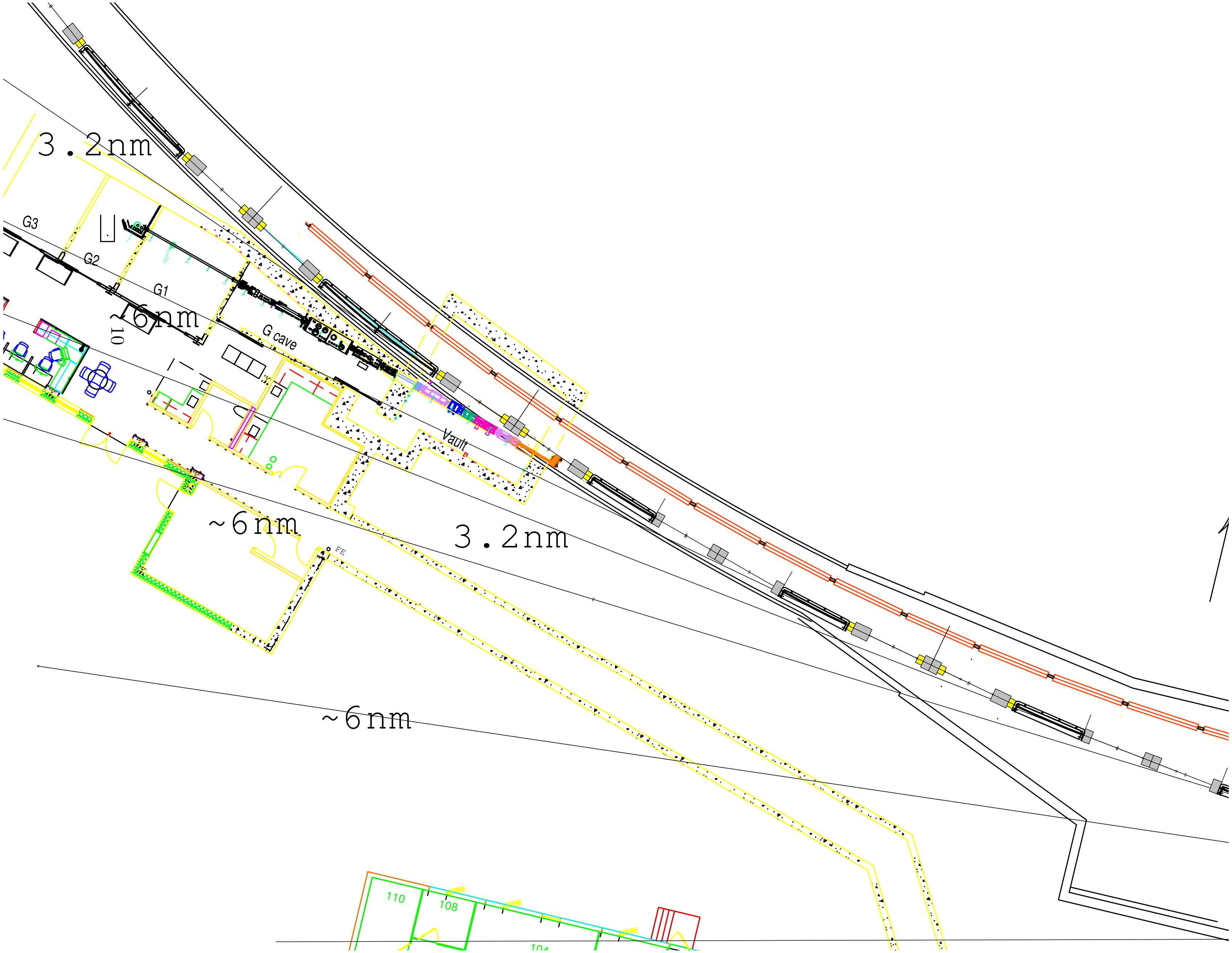

3.2nm
G3
G2
G1
~6nm
~10
G cave
Vault
~6nm
3.2nm
~6nm
110
108

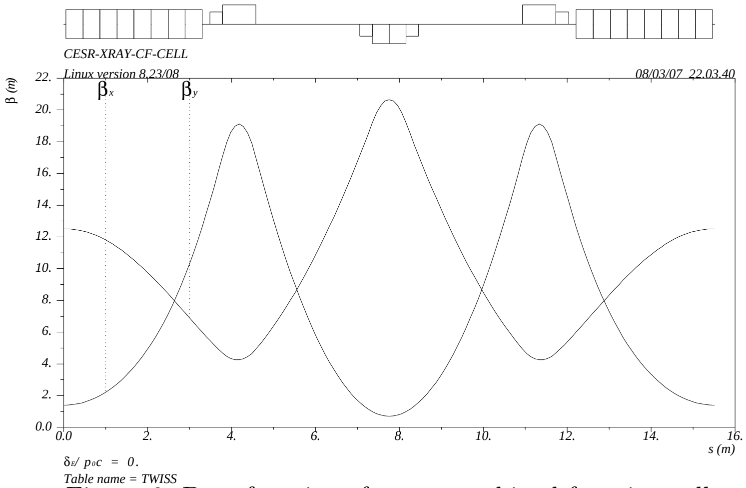

Figure 6: Beta functions for one combined function cell.

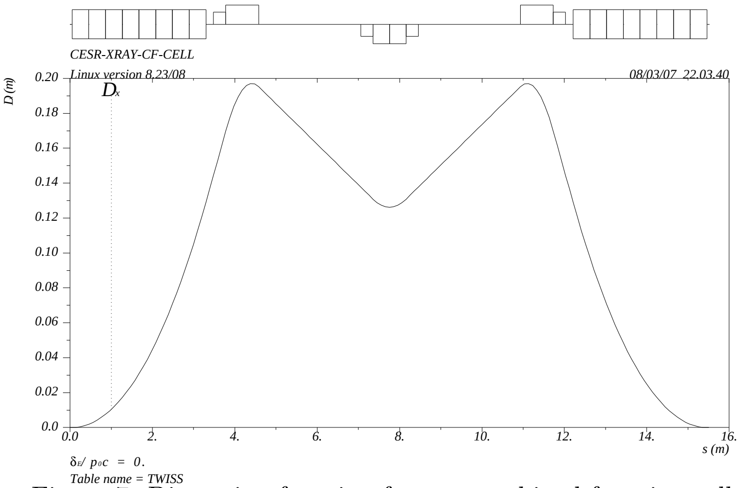

Figure 7: Dispersion function for one combined function cell.

2 Transverse Lattice Functions and Parameters

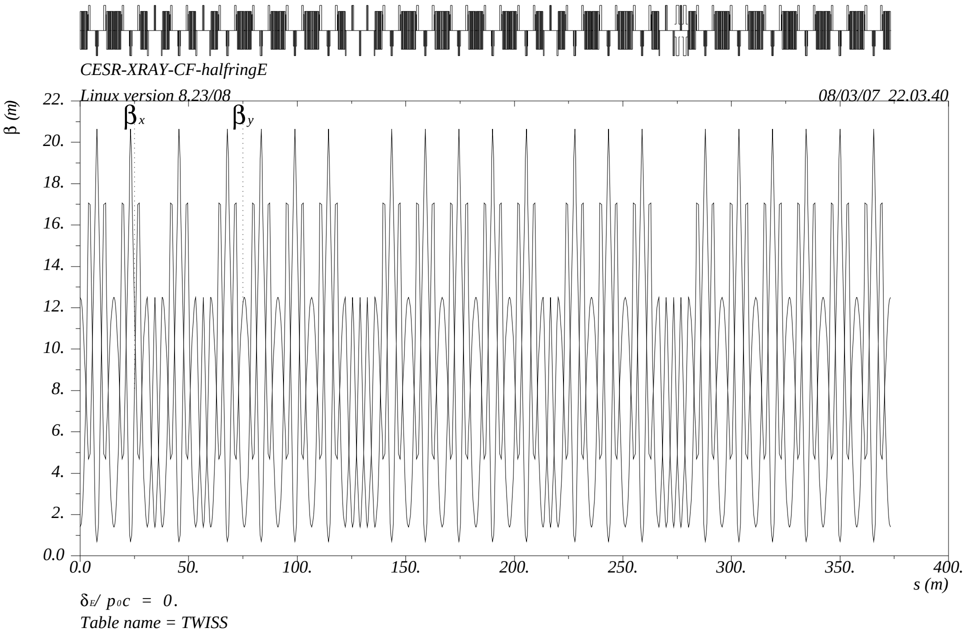

Figure 8: Beta functions for most of East half ring.

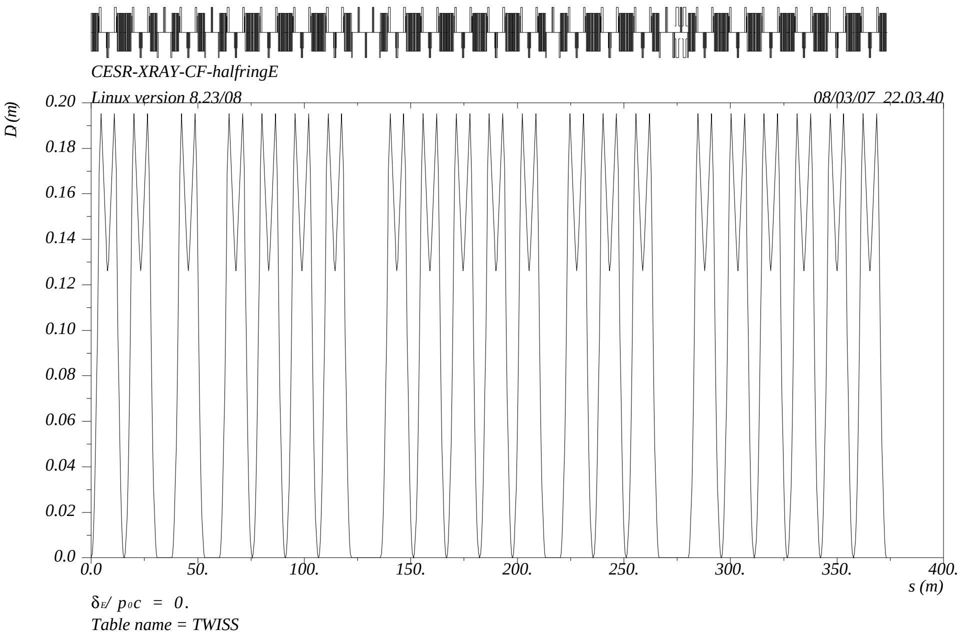

Figure 9: Dispersion function for most of East half ring.

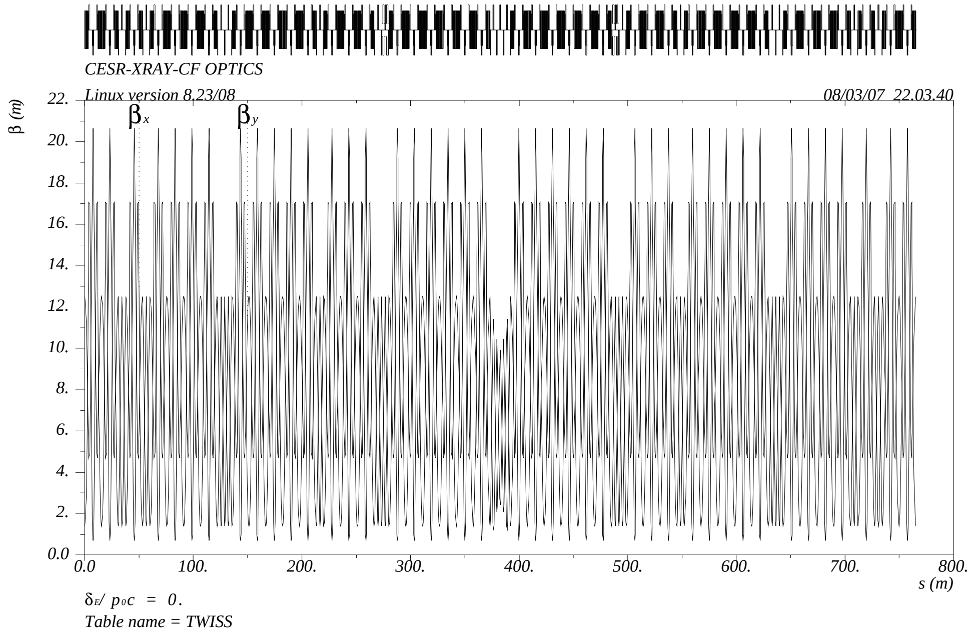

Figure 10: Beta functions for full ring with combined function optics.

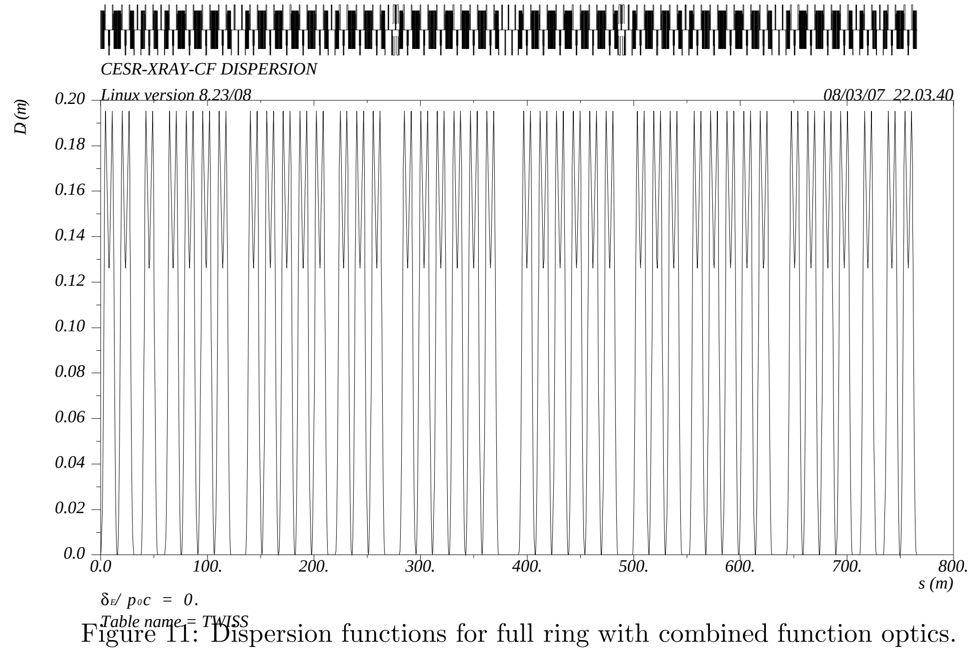

Figure 11: Dispersion functions for full ring with combined function optics.

Table 1: Parameters for option **A**, combined function bends.

parameter	unit	**A**
number of bend cells		42
number of FODO cells		14
number of half bends		33
number of full bends		18
L_b	m	6.498
θ	rad	$\pi/21$
ρ	m	43.4359
visible long $D=0$ und. straights	m	1 @ 6*lmatch=14.0
vis. med. len. $D=0$ und.straights	m	1 @ 4*lss=10.3
visible short $D=0$ und. straights	m	4 @ 2*lss=5.2
visible utility straights	m	9 @ 2*ld1=4.9
free medium $D=0$ straights	m	2 @ 4*lss=10.3
free short $D=0$ straights	m	2 @ 2*lss=5.2
free utility straights	m	33 @ 2*ld1=4.9
r.f. straight	m	1 @ 4*lss=10.3
l_{q1}	m	0.8
l_{q2}	m	0.4
$l_{fullssquad}$	m	0.8
l_{sext}	m	0.3
$l_{bend\ cent.\ qb}$	m	0.05
$ld2$	m	0.182371
$ld1$	m	2.474328
lss	m	2.592504
N_{q1}		42
N_{q2}		84
$N_{q_{ss}}$		16
$N_{q_{ss}/2}$		32
`k1[q1]`	1/m	-0.454399*8/6
`k1[q2]`	1/m	0.708326*8/6
`k1[qss]`	1/m	0.650530*8/6
`k1[b], kl1[qb]`	1/m	-0.07
$lmatch$	m	2.336833
`k1[q1match]`	1/m	-0.712230*8/6
`k1[q2match]`	1/m	0.645351*8/6
`k1[q3match]`	1/m	-0.642844*8/6
`k1[q4match]`	1/m	0.594663*8/6
tunes, ν_x, ν_y		37.274/17.364
tunes, thin el. foc.		37.281/17.375
`k2[S1], k2[S2]`	m^{-3}	-11.0/14.6
β_{x0}, β_{y0}, D_0	m	1.40/12.5/0.0
$<\mathcal{H}>$	mm	4.72
J_x		1.25
ϵ_x@5GeV	nm	3.2

3 Longitudinal Parameters

The lattice is "isomagnetic", meaning that, everywhere the B field is nonvanishing it has the same value. Assuming $\mathcal{E}_e = 5.0\,\mathrm{GeV}$, we have

$$\rho = 43.4359\,\mathrm{m}, \quad \text{and} \quad B = 0.3840\,\mathrm{T}. \tag{1}$$

The energy radiated per electron per turn is then given by

$$U_0 = 1.273\,\mathrm{MeV}. \tag{2}$$

The characteristic x-ray energy is

$$u_c = 6.384\,\mathrm{KeV}. \tag{3}$$

The longitudinal slip factor is

$$\eta_0 \equiv \frac{1}{\gamma_t^2} = 3.45 \times 10^{-4}, \tag{4}$$

where γ_t is the so-called "transition-γ and the longitudinal phase advance per turn is given by

$$\mu_s^2 = \frac{\mathcal{C}}{c}\,\omega_{\mathrm{RF}}\eta_0\,\cos\phi_0\,\frac{\hat{V}}{\mathcal{E}_e}, \quad \text{or} \quad Q_s = \frac{\mu_s}{2\pi} = 0.0090, \tag{5}$$

where $\mathcal{C} = 765\,\mathrm{m}$, $\omega_{\mathrm{RF}} = 2\pi \times 500\,\mathrm{MHz}$, $\hat{V} = 6\,\mathrm{MeV}$ and, for the time being, $\cos\phi_0 = 1$. For this calculation it has been assumed that the RF accelerating cavities are in one of the "not visible" medium length straight sections. The performance will be unaffected by this choice.

For separate function lattices, Sands' $\mathcal{D} << 1$, and the fractional energy spread is given by

$$\sigma_\delta = 0.813\sqrt{\frac{u_c}{(2+\mathcal{D})\,\mathcal{E}_e}} = 0.65 \times 10^{-3}. \tag{6}$$

This will have to be corrected for the effect of the (relatively weak) combined function bend magnets. The bunch length (needing similar correction) is given by

$$\sigma_{ct} = \frac{\mathcal{C}D_0}{\mu_s}\,\sigma_\delta = 2.92\,\mathrm{mm}. \tag{7}$$

Expressed as a time this is

$$\sigma_t = \sigma_\delta = 9.7\,\mathrm{ps}. \tag{8}$$

Though this is some ten times shorter than the x-ray pulses from CESR it is still a long way from the sub-picosecond "fast timing" frontier the ERL is intended to investigate. (The NSLS II proposal does, however, suggest some experiments exploiting the timing capabilities of bunches of this duration.)

As a matter of fact, the short bunch length will probably be a major nuisance, both because of excessive higher mode power dissipation and excessive particle loss through Touschek scattering. It is very likely, therefore, that one will plan to have a third harmonic bunch lengthening RF cavity right from the start.

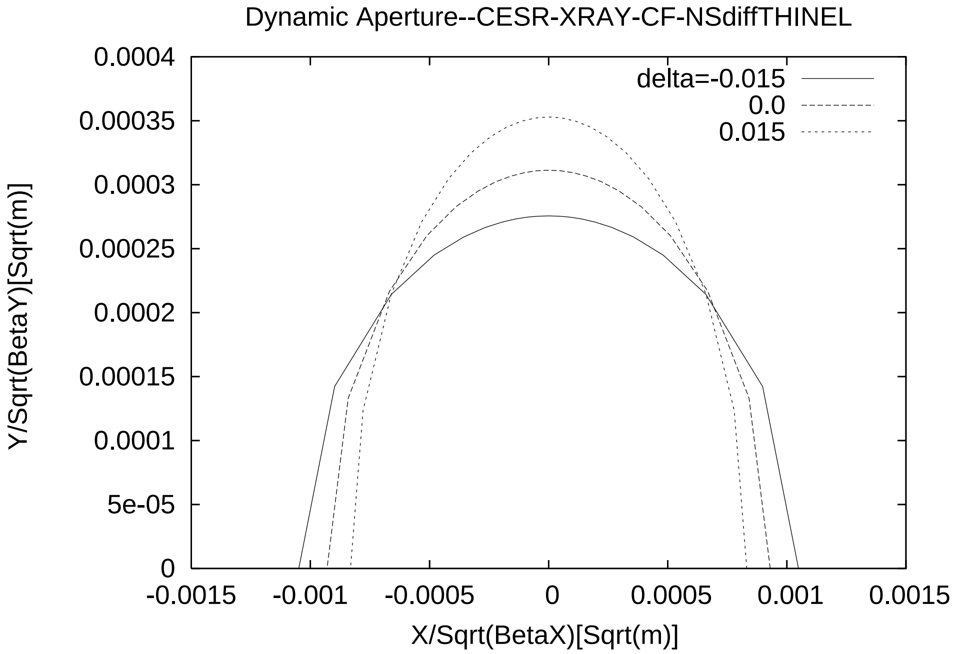

Figure 12: Dynamic aperture for combined function design for fractional off-momentum values of -0.015, 0, and $+0.015$, which corresponds to $\pm 20\sigma_\delta$.

4 Dynamic Aperture

Only the most preliminary investigation of dynamic aperture has been attempted so far. The results are shown in Fig. 12 for fractional off-momentum values out to $15\sigma_\delta$. On this range the curves mainly just superimpose on one another. Curiously, with synchrotron oscillations turned off the aperture is approximately constant over a momentum range far greater than has been typical for CESR. This seems to be a consequence of the very small dispersion values.

With nothing but the global constraints mentioned earlier the tunes come out $Q_x = 37.27$, $Q_y = 17.36$. No attempt has been made to adjust these values to alter the dynamic aperture. For one of the lattice options (separated function) analysed in the earlier report, Dave Rubin performed lattice calculations that agreed in detail concerning the optics. He also investigated dynamic aperture and, especially after adjusting for more optimal tunes, found fully satisfactory dynamic aperture. His predicted emittance was also larger by a factor 1.37 than the value given in that report. After finding a bug in the (report's) calculation the agreement became excellent. Dave has not yet performed similar studies on the lattice discussed in this report.

With the scales of Fig. 12 being scaled as $x/\sqrt{\beta_x}$ and $y/\sqrt{\beta_y}$, the plotted maximum amplitudes are applicable at arbitrary points in the lattice. This also makes the values directly comparable to ϵ_x and ϵ_y. Comparison is easiest at a point for which $\beta_x = 1\,\mathrm{m}$. As it happens, this is (roughly) true at magnet centers and sextant ends for the proposed lattice. A range $-0.001\,\mathrm{m} < x/\sqrt{\beta_x} < 0.001\,\mathrm{m}$ then corresponds to a range

$$0 < \epsilon_x < 10^{-6}\,\mathrm{m}. \tag{9}$$

According to the data of Fig. 12 the vertical acceptance is some three times smaller than the horizontal. Usually apertures are quoted in units of beam sigmas. Expressed that way, with the aperture range being given by Eq (9) the aperture would be $\sqrt{0.8e-6/3.2e-9} = 16$ sigmas. This is ample for long lifetime of the beam at equilibrium but small enough to make injection efficiency uncertain.

The beam size of the beam extracted from the synchrotron at 5 GeV is about 2 mm at $\beta_x = 40$ making its horizontal emittance about $10^{-7}\,\mathrm{m}$. (This has to be checked and refined.) Since this is comparable with the acceptance, injection should be OK, but possibly not great.

5 Brilliance

The master formula governing the brilliance of the x-ray beam produced by electron beam current I from the fundamental $n = 1$ undulator resonance, in an undulator having N_w periods, with undulator parameter K (assumed less than 1), due to Krinsky[9] and possibly others, is[1],

$$\mathcal{B}_1 = \frac{2\times 10^{18}\, I(\mathrm{A})}{\epsilon_x(\mathrm{nm})\epsilon_y(\mathrm{nm})}\,\frac{N_w\, K^2}{1+K^2/2}\,\frac{\mathrm{photons}}{\mathrm{s\ mm^2\ mr^2\ 0.1\%BW}}. \tag{10}$$

Here ϵ_x and ϵ_y are unnormalized emittances. This formula describes an $n = 1$, monochromatic x-ray beam whose wavelength depends, among other things, on the undulator period λ_w.[2]

Values of $\mathcal{B}_1$ for various storage rings are shown in Table 2. Since the electron energies of the various light sources are different their optimal energies are also different. Note though, that $\mathcal{B}_1$, as given by Eq. (10), is independent of $\mathcal{E}_e$. To (somewhat dubiously) simplify the comparison of the different rings it is assumed they all use undulators with wavelength $\lambda_w = 5\,\mathrm{cm}$ and then to calculate $\mathcal{B}_1$ at the photon energy of the fundamental peak of the undulator spectrum from that undulator. *Typically* photons of energy higher than this are actually used, for example photons produced on the $n = 3$ undulator peak. The second to last row of Table 2 gives the photon energy for that case. The brilliances given in the

[1] The functional dependences in Eq. (10) are not controversial, at least for some conventional beamline designs, but the multiplying factor may vary by a factor of two or so, depending on assumptions.

[2] Qualification: Eq. (10), especially its only-linear dependence on N_w, depends on relations between the angular spreads of the electron beam and the produced photon cone angle. These relations are likely to be different for horizontal and vertical emittances in different ranges of interest.

Table 2: Comparison of brilliance $\mathcal{B}_1$ for various storage rings are given in the final row in the units of Eq. (10), which has been used to calculate $\mathcal{B}_1$. Standard undulator parameters λ_w=0.05 m and K=1 are assumed in all cases so the number of poles is $N_w = L_{\text{undulator}}/0.05$. Columns headed by **CESR'** refer to the design analysed in this report. The entries in the row labeled $\mathcal{E}_{\gamma,dl}(\epsilon_y)$ (giving the energy above which the quoted brilliance is fully-effective, i.e. not diffraction-limited) and *characteristic* photon energies (labelled $\mathcal{E}_3$ @ 0.05 m) are explained in the text. This table does not properly reflect the fact that, at NSLS II, they expect to be able to use undulators with λ_w as short as 14 mm to get high x-ray energies in spite of the low electron energy.

		NSLS II	**CESR'**	**CESR'**	Cornell -ERL	ESRF	APS	SPRING -8
aspect ratio	units	flat	flat	round	round	flat	flat	flat
$\mathcal{E}_e$	GeV	3.0	5.0	5.0	5.0	6.0	7.0	8.0
ϵ_x	nm	1.5	3.2	1.6	0.2	4.0	2.8	3.4
ϵ_y	nm	0.008	0.032	1.6	0.2	0.04	0.028	0.034
$\mathcal{E}_{\gamma,dl}(\epsilon_y)$	keV	49	12.4	0.34	2.0	9.9	14.1	
$L_{\text{undulator}}$	m	5	10	10	10	2.0	4.0	
I	A		0.5	0.5	0.1	0.2	0.1	0.1
$\mathcal{E}_3$ @ 0.05 m	keV	5.13	14.2	14.2	14.2	20.5	27.9	36.5
$\mathcal{B}_1$	$\times 10^{20}$		13	0.53	6.7	2.5	5.1	
actually achieved						2.2		2

last row *do not* correspond precisely to these energies; they are less, typically by a factor of two or so which should, however, be more or less common to all columns.

The flat beam brilliances only become fully effective for photons of wavelength less than $\pi\epsilon_y$. In the row labeled $\mathcal{E}_{\gamma,dl}(\epsilon_y)$ the (approximate) energy above which the full brilliance at the given value of ϵ_y becomes applicable is given. In all cases except NSLS II the full calculated brilliance is applicable at the *nominal* photon energy $\mathcal{E}_3$ given in the second last row.

A beam current 0.5 A is assumed, By retaining the same vacuum tube dimensions as are currently used in CESR, one expects the maximum beam current to at least match the maximum total current that has been obtained in CESR. (This may be compromised somewhat if the combined function vacuum chamber height has to be reduced from its current two inch value.) However, because of reduced beam lifetime due to the Touschek effect, it is expected that full energy injection superior to what is available from the Wilson synchrotron may be necessary for high current operation. As explained earlier, ultrafast timing experiments will also only become possible with such an injector. It is expected (though the designs have not been performed) that single turns of ultrashort bunches can be conveyed around the ring and delivered to any of the beamlines (though not simultaneously to all lines.)

6 Costs

Table 3 gives cost breakdowns for the CESR upgrade. All costs in this tables are expressed as what the cost *would have been* assuming the parts were acquired in 1978 at the same time that all the other components were being built. The nominal inflation factor from 1977 to 2006 is 3.3. It is not clear whether accelerator components inflate at the nominal rate but, if they do, then all costs in the tables need multiplication by 3.3 to bring them up to date.

The largest unincluded costs are (obviously) the costs of instrumenting the x-ray lines. Obviously these costs have to be estimated, justified, and born by the scientific experiments using the beam lines. Even apart from these beam line costs, many wise local experts are of the opinion that the true inflation figure should be far greater than the nominal 3.3 value. If one accepts this it just strengthens the case for the proposed upgrade. For consistency, one should assess the replacement value of the existing Wilson laboratory infrastructure using the same units.

Just one of the many rings coming on line soon, DIAMOND in England, has cost close to half a billion dollars. For soft x-rays its brilliance will be comparable with the upgraded CESR but, because of its only 3 GeV energy, its brilliance will be much less for hard x-rays. (This is both because of the Touschek effect and the physics of undulator radiation.) This is one basis for the statement in the abstract that the proposed upgrade represents "great value for a commodity in great demand".

References

[1] R. Talman, *Accelerator X-Ray Sources,* Wiley-VCH Verlag, Weinheim, 2006

[2] Design Report, Cornell Electron Storage Ring, April, 1977

[3] S. Turner, editor, *1996 CERN Accelerator School: Synchrotron Radiation and Free Electron Lasers*, CERN Yellow Report 98-04, 1998

[4] A. Ropert, *Lattices and Emittances,* in CERN Yellow Report 98-04, S. Turner, editor, 1998

[5] D, Brandt, editor, *2005 CERN Accelerator School: Synchrotron Radiation and Free Electron Lasers*, CERN Yellow Report, CERN-2005-012

[6] R. Chasman and K. Green, *Preliminary Design of a Dedicated Synchtotron Radiation Facility,* IEEE Trans. Nucl. Sci., NS-22, 1765 (1975)

[7] H. Grote and F. Iselin, *The MAD Program (Methodical Accelerator Design) Version 8.19, User's Reference Manual,* CERN/SL/90-13 (AP), 1996

[8] H. Wiedemann, *Brightness of Synchrotron Radiation from Electron Storage Rings,* Nucl. Instr. Meth., 172 (1980)

Table 3: Design **A** (combined-function full chevrons) costs estimated as they would have been in 1977 during initial CESR construction. Cornell in-house labor not included. [2] Also not included are: RF modification; transfer line modification; extra cooling capacity; conventional construction. Also any equipment, such as undulators, specific to x-ray beam lines. Element counts have not yet been updated to reflect the changes needed to restore closure after giving up North/South symmetry of the lattice.

Component	part	identifier	number	unit cost $K	total cost $K
Bends	new half bend		12	6	72
	new full bend		36	6.5	234
	bus and hook-up				54
Quads	new coil, existing quad	q_2	84	1	84
	new full quad	q_1	42	2.5	105
	new full quad	q_{ss}	16	2.5	40
	new half quad	$q_{ss}/2$	32	2	64
	power supplies		90	1	90
Sextupoles	new sext. + p.s.	$s2$	84	1.6	134
	possible replacements	$s1$	84	1.6	0
Beam monitoring					383
Supports					100
Vacuum					1000
Total					2360

[9] S. Krinsky, article *Fundamentals of Hard X-Ray Synchrotron Radiation Sources*, in *T*hird Generation Hard X-Ray Synchrotron Radiation Sources, D. Mills editor, John Wiley, New York, 2002

[10] I. Bazarov and C. Sinclair, PRST-AB, **8**, 034202 (2005)

[11] R. Brinkmann et al., TESLA Technical Design Report, Part II, DESY 2001-011, ECFA 2001-209

[12] M. Borland et al., SLAC Report-402 (1991)

[13] R. Sheffield et al., PAC 95, p. 882

[14] D. Trbojevic and E. Courant, *Low emittance lattices for electron storage rings, revisited,* in Proc. EPAC94, p. 1000

[15] K. Steffen, *High Energy Beam Optics,* Interscience Publishers, New York, 1965, p. 17

[16] N. Malitsky and R. Talman, *Accelerator Simulation Using the Unified Accelerator Libraries (UAL)*, U.S. Particle Accelerator School, Ithaca, 2005. Available at `http://www.ual.bnl.gov`

[17] H. Bruck, *A*ccélérateurs Circulaires de Particules

[18] C. Bocchetta, *L*ifetime and Beam Quality in CERN 98-04

[19] Y. Miyahara, IEEE Trans. Nucl. Sc., **32**, 3821 (1985)

[20] L.Mandel and E. Wolf, *Optical Coherence and Quantum Optics*, Cambridge University Press, p.269, 1995